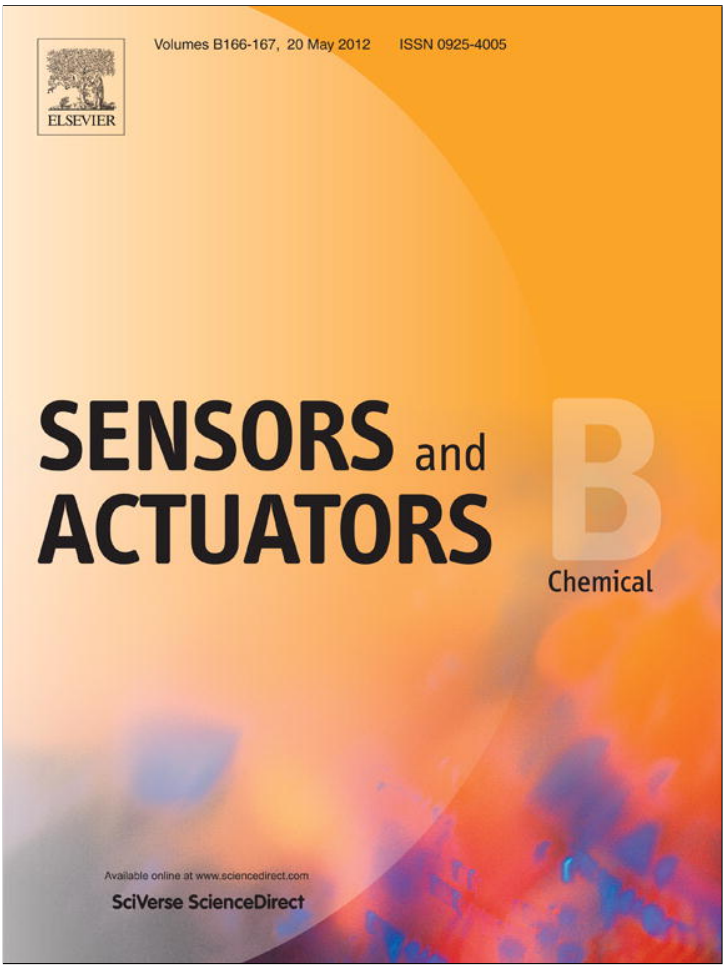

Sensors and Actuators B 166–167 (2012) 777–786

Contents lists available at SciVerse ScienceDirect

Sensors and Actuators B: Chemical

journal homepage: www.elsevier.com/locate/snb

Excimer-laser deinsulation of Parylene-C coated Utah electrode array tips

Je-Min Yoo[a,b,*], Asha Sharma[b], Prashant Tathireddy[b], Loren W. Rieth[b], Florian Solzbacher[b], Jong-In Song[a,**]

[a] Department of Nanobio Materials and Electronics, Gwangju Institute of Science and Technology, Gwangju 500-712, Republic of Korea
[b] Department of Electrical and Computer Engineering, University of Utah, Salt Lake City, UT, United States

ARTICLE INFO

Article history:
Received 2 June 2011
Received in revised form 19 March 2012
Accepted 27 March 2012
Available online 2 April 2012

Keyword:
UEA
Parylene
Laser deinsulation
Photoablation
Excimer laser

ABSTRACT

Utah electrode arrays (UEAs) are highly effective to measure or stimulate neural action potentials from the central or peripheral nervous system. The measured signals can be used for applications including control of prosthetics (recording) and stimulation of proprioceptive percepts. The UEAs are coated with biocompatible Parylene-C, and the electrode tips are deinsulated to expose the active electrode coated with sputtered iridium oxide films (SIROFs) to transduce neural signals. In conventional UEA technology, the electrode tips are deinsulated by poking the electrodes through aluminum foil followed by an oxygen plasma etch of the exposed areas. However, this method suffers from lack of uniformity and repeatability and it is time consuming. We focus on laser tip-deinsulation technology that can provide a repeatable, uniform, and less time consuming tip exposure for UEAs. The laser deinsulated SIROF area is characterized by X-ray photoelectron spectroscopy (XPS), scanning electron microscope (SEM), atomic force microscope (AFM), and by measuring the impedance of the exposed sites. The value of impedance and XPS peaks showed that the Parylene was clearly removed. The damage induced by laser irradiation on the SIROF film was also investigated to understand the selectivity of laser deinsulation. Thicker SIROF films showed better resistance to fracture. The results indicate that laser deinsulation is an effective method to etch Parylene films.

1. Introduction

Neural interfaces for chronic implantation need to be encapsulated by a biocompatible material to protect the device from the harsh physiological environment. In addition, the encapsulation material must be biocompatible in contact with the neural tissue in the vicinity of the device. Parylene-C, which has a polymer structure as presented in Fig. 1, is a representative material for encapsulation in biomedical implants and has good adhesion, uniformity, electrical insulation, and biological and chemical inertness, is non-toxic to body tissue [1–3].

Neural recording and stimulation require the removal of the Parylene from the active electrode tips of the UEA to facilitate transduction [4]. In very early designs, the recording tips of the microelectrodes were exposed either by using a heating element to melt back the insulation or by a high-voltage arcing technique [2]. The heating method usually led to the breakdown of the insulation near the tip after implantation. The high voltage arcing technique resulted in poor adhesion of the Parylene insulation at the tips and caused tiny fractures along the electrode shaft, which decreased the impedance values. In addition, these methods made it difficult to control the size of the tip exposure. Several other methods, such as chemical etching, cannot be used because Parylene is inert to most solvents. Therefore, dry etching processes are currently considered the most suitable method, and these include plasma etching, ion reactive etching, and deep reactive etching [5].

Oxygen plasma etching is the standard method to remove Parylene from the electrode tip in UEA manufacturing [6]. Both the photoresist and the aluminum foil mask with oxygen plasma etching have been investigated in UEA technology [7–9]. However, the photoresist etching mask changes the surface properties of the Parylene. Therefore, poking the electrode tips through an aluminum foil to the desired exposure length for deinsulation of the Parylene has been adopted as a regular masking procedure in UEA technology. However, the poking of an aluminum mask is a time consuming process that is not practical on a production scale, and it also has an inherent problem of non-uniformity and poor repeatability leading to a large variation in the impedance values. Moreover, the foil mask cannot be used for more complex geometries, such as variable height electrodes.

* Corresponding author at: Department of Electrical and Computer Engineering, University of Utah, 50S Central Campus Drive, MEB 1690, Salt Lake City, UT 84112, United States. Tel.: +1 801 581 6941; fax: +1 801 581 5281.
** Corresponding author. Tel.: +82 62 715 2208.
E-mail addresses: Je-Min.Yoo@utah.edu (J.-M. Yoo), jisong@gist.ac.kr (J.-I. Song).

0925-4005/$ – see front matter © 2012 Elsevier B.V. All rights reserved.
http://dx.doi.org/10.1016/j.snb.2012.03.073

UU IR Author Manuscript

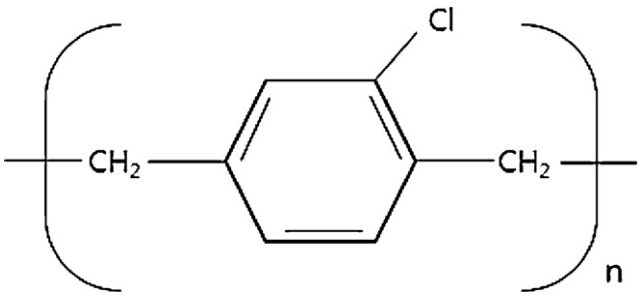

Fig. 1. The structure of Parylene-C.

To overcome the shortcomings of an aluminum foil mask, deinsulation using a laser is investigated as an appropriate alternative. Laser ablation of Parylene has been used since the early 1990s [10]. Laser deinsulation has also been demonstrated to remove Parylene from biomedical microelectrodes based on Pt tips [11,12], and to ablate micron-thick Parylene films from a copper surfaces [13].

There are two primary mechanisms for laser etching, vaporation and photoablation, which result in removal of surface layers [14]. To use the laser photoablation method for Parylene deinsualtion from UEA tips, several processing parameters, for example, laser wavelength, pulse duration, the number of pulses, and fluence, need to be optimized. In this study, we used the laser ablation method for deinsulating the Parylene-coated iridium oxide tips of the UEA. The trade-off between the fluence and the number of pulses was an important consideration for selective photoablative removal of Parylene without leaving any cracks or damage in the iridium oxide active electrode surfaces. Using a KrF (248 nm) excimer laser appears to be a useful ablation method due to a strong absorption characteristic of the Parylene as well as the iridium oxide film in the UV region below the wavelength of 280 nm.

We first investigated the laser ablation of the Parylene-coated iridium oxide film deposited on flat silicon substrates to study the influence of the laser and characterize the laser ablated iridium oxide surfaces by scanning electron microscopy (SEM), atomic force microscope (AFM), and X-ray photoelectron spectroscopy (XPS). Based on the optimization of the laser parameters on planar surfaces, we implemented the laser ablation method to deinsulate the Parylene from the tips of 3-D Utah electrode array.

2. Experiment

2.1. Fabrication of planar structures and microelectrode arrays

The flat substrates prepared for initial optimization of the laser deinsulation parameters consisted of film stacking similar to the Utah electrode array. The samples were prepared using *p*-type (100) single crystal silicon wafers. Titanium (50 nm), followed by iridium oxide (400, 800 and 1100 nm) were deposited on the silicon

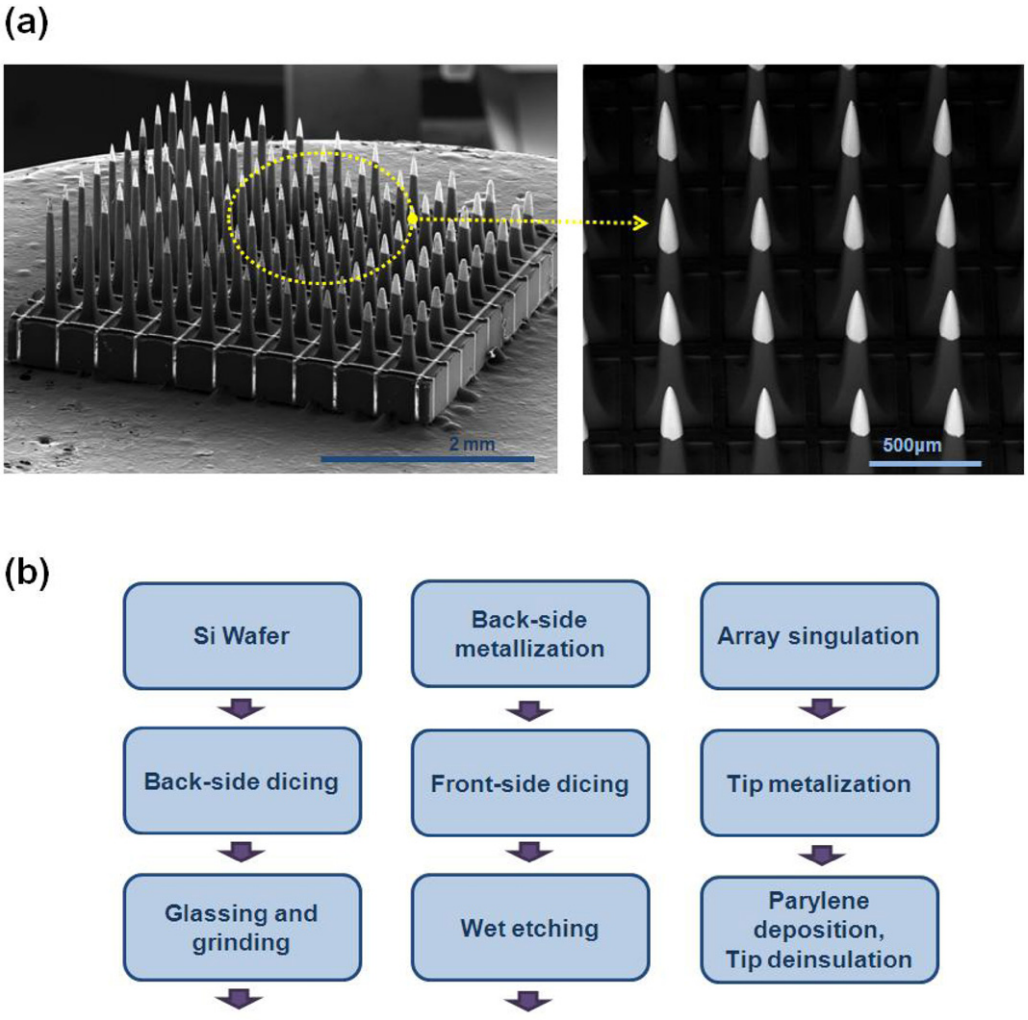

Fig. 2. (a) Scanning electron micrograph of UEAs (left) and the backscattered image of the electrode array in detail (right) and (b) schematic view of the process flow for wafers-scale fabrication of the Utah electrode array.

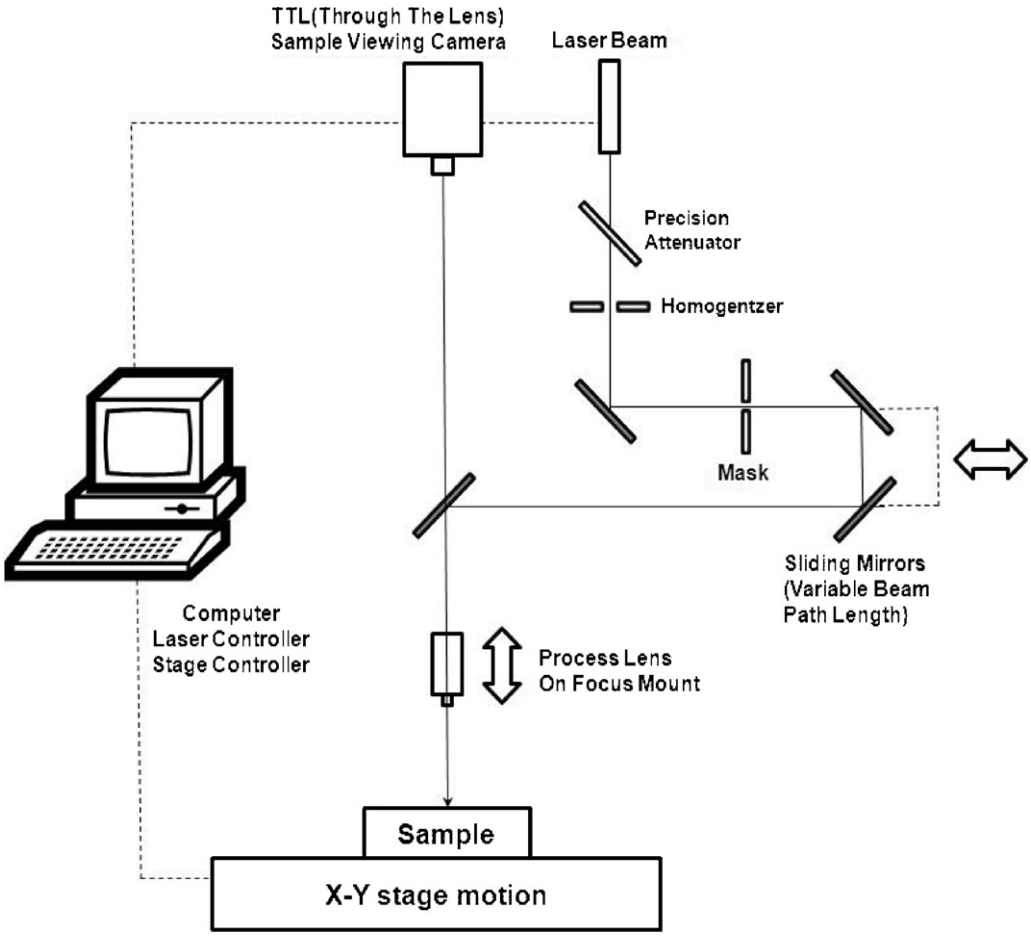

Fig. 3. Schematics diagram of the laser ablation system.

substrates by DC and Pulsed-DC sputter deposition, respectively (TMV Super Series SS-40C-IV Multi Cathode Sputtering system). The titanium acts as an adhesive layer and was deposited in Ar ambient with flowing of 150 sccm at a chamber pressure of 20 mTorr and sputtering power of 90 W for 5 min. The titanium target was 99.6% pure, 3 in. in diameter and 0.125 in. in thickness (KurtJ Lesker, Pittsburgh, PA). SIROF was deposited in Ar and O_2 plasma with both gases flowing at the rate of 100 sccm. The sputtering power was 100 W with deposition pressure of 10 mTorr. The deposition rate was 10 nm/min. The pulse width and frequency were 2016 ns and 100 kHz, respectively. The iridium target was 99.8% pure, 3 in. in diameter and 0.125 in. in thickness (KurtJ Lesker, Pittsburgh, PA). Three different thicknesses of iridium oxide films were deposited on flat substrates in order to investigate film damage from the laser. Annealing (Lindberg Annealing Furnace, 375 °C using 98% Ar and 2% H_2 forming gas) was performed to improve the adhesion between the deposited films and the substrate, and aid in the formation of Ohmic contacts. Parylene (3 μm) film was deposited by chemical vapor deposition using a Paractech 3000 Labtop deposition system. To improve the chemical adhesion between the Parylene and the underneath film, 0.5% Silquest A–174 silane was used. Finally, the Parylene film was removed from the active area by the laser system (Optec MicroMaster Excimer Laser, KrF 248 nm).

The UEA is a 3-D silicon-based structure consisting of a 10 × 10 array of tapered silicon electrodes with a length of 1.5 mm and pitch of 400 μm between tips as shown in Fig. 2(a). The detailed SEM image on the right presents several electrodes just after tip metallization which shows the connections to iridium oxide film that form the active surface. Fig. 2(b) is the schematic view of the process flow for wafers-scale fabrication of UEAs. To make the UEAs, a 2 mm thick, p-type, c-Si (1 0 0) wafer with the diameter of 75 mm and a resistivity of 0.01–0.05 Ω·cm was prepared as substrates. Back-side dicing, glassing and grinding were needed to form the back side metal pad for wire bonding. Front-side dicing and wet etching were then used to shape the electrodes. Then, array singulation, tip metallization and Parylene deposition were performed to complete the devices. During the tip metallization, titanium and iridium oxide were deposited by DC and Pulsed-DC sputter deposition, respectively, and annealed in a way similar to that described for the planar substrates. For the last step, tip deinsulation was carried out. The fabrication of UEAs is described elsewhere in detail [7,15].

2.2. Excimer laser system and optical layout description

The laser deinsulation system used in this study includes an excimer laser, sophisticated beam delivery optics, a precision sample motion stage, and a computer with a flexible control software as shown in Fig. 3. The wavelength of the laser is 248 nm (KrF) which is capable of photoablating the Parylene films. The laser operates in a pulse mode, typically pulsing at a rate of 100 Hz. Pulses are 5–6 ns in duration. The fluence can be controlled by laser energy.

This system uses projection optics where the laser beam is passed through a circular mask, and then was demagnified and focused on the sample. A circular mask was used because the electrode base is circular. The sample for laser deinsulation was mounted on a vacuum chuck. The sample motion stage had a

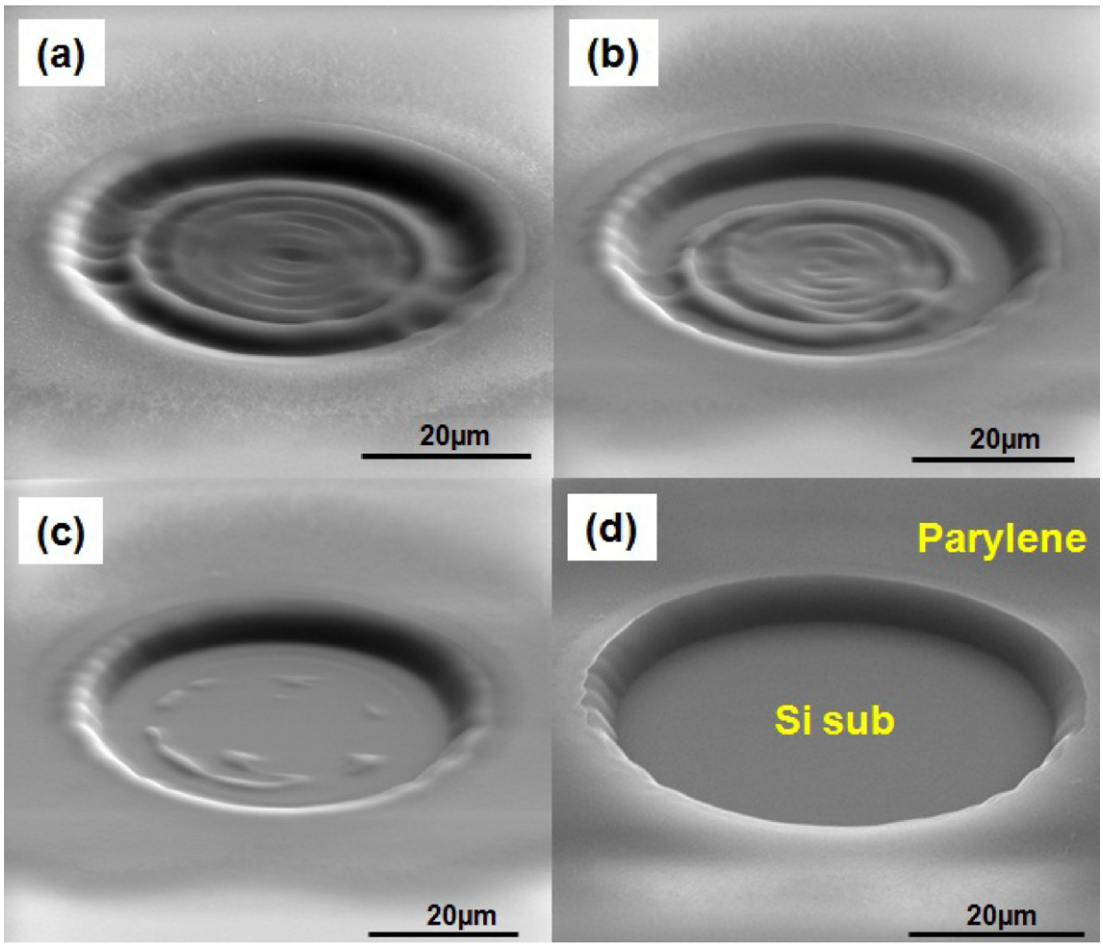

Fig. 4. 30° tilted scanning electron micrographs (SEM) of the circles on a silicon substrate after laser ablation with 1000 mJ/cm^2: (a) 10 pulses, (b) 20 pulses, (c) 30 pulses and (d) 100 pulses.

resolution of 1 μm in *x* and *y* directions. The deinsulated area of the tip depends not only on the mask size but also on the laser fluence and the number of laser pulses. After optimization of all these factors for the desired tip exposures on the UEAs, a circular mask with the diameter of 550 μm and a process lens with a demagnification of 7.3 and a working distance of ~10 cm between sample and process lens were used in our experiments.

Additionally, monitoring the sample is also important for deinsulation of electrode tips precisely in μm scale. Therefore, a real-time observation by visible imaging was used to control the deinsulation process. The laser ablation system used in this study had dual-camera vision including an off-axis camera for general overview and a high magnification through the lens (TTL) image in windows on a flat screen monitor. When the sample was in focus on the CCTV, the UV was automatically in focus on the sample. The laser system has independent light sources, including a highlighter for optimum contrast on the sample. This was helpful in finding the tip location.

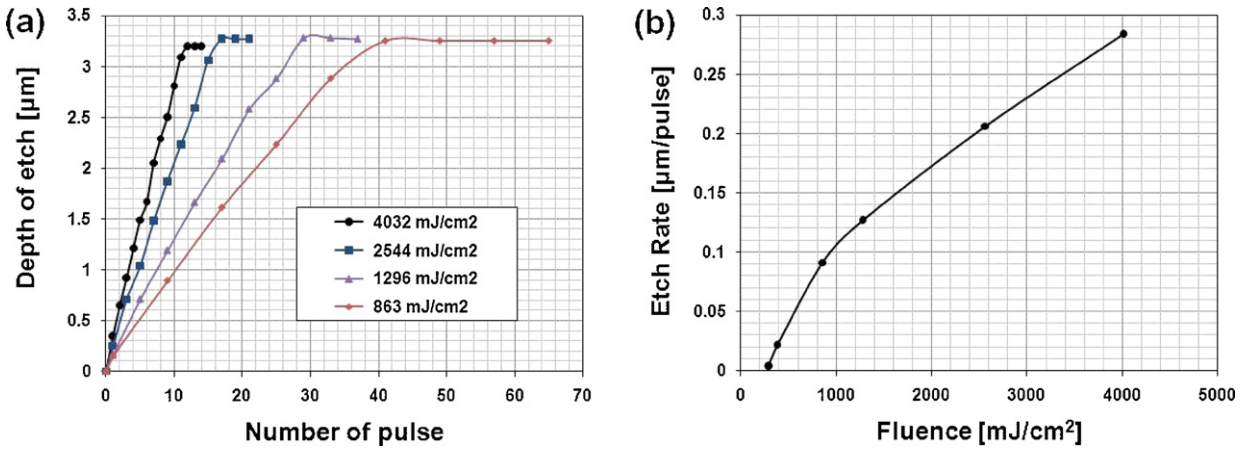

Fig. 5. (a) The etch depth of the Parylene as a function of the number of laser pulses and (b) the Parylene etch rate by as a function of the fluence.

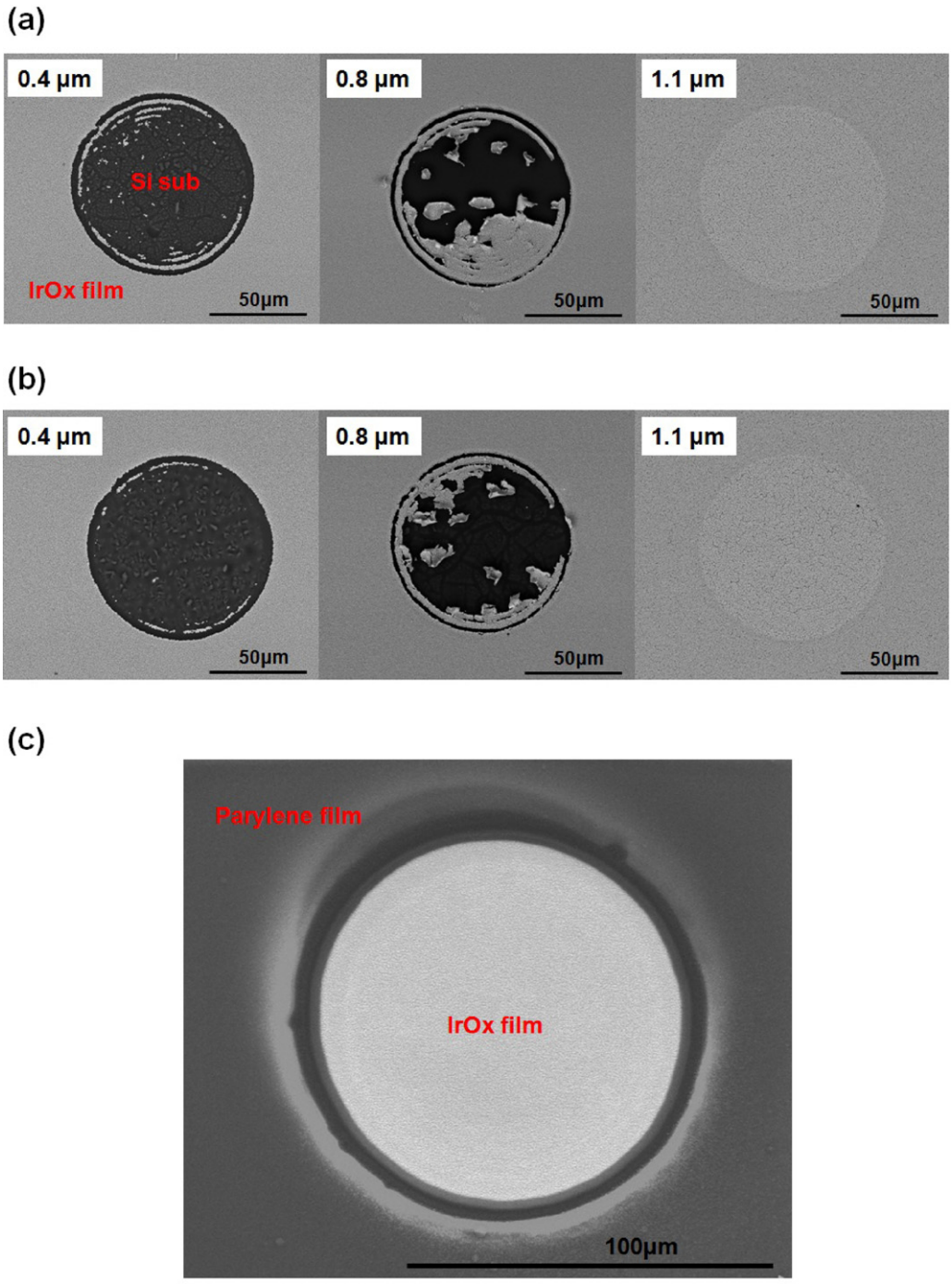

Fig. 6. (a) SEM images (backscattering images) for films with three different thicknesses (0.4 μm, 0.8 μm, and 1.1 μm) exposed to a single laser pulse with 1680 mJ/cm^2 fluence for investigation of iridium oxide film fracture tendency, (b) SEM images for films with three different thicknesses (0.4 μm, 0.8 μm, and 1.1 μm) exposed to 100 laser pulses with 1680 mJ/cm^2 fluence and (c) SEM image of the laser ablated hole on a Parylene-coated iridium oxide film.

2.3. Surface, chemical, and electrical characterization of laser deinsulated electrodes

The surface morphology and roughness before and after laser deinsulation were examined by scanning electron microscopy (SEM) using an FEI Quanta SEM and a Digital Instruments atomic force microscope (AFM). Chemical analysis of the deinsulated spots was performed by X-ray photoelectron spectroscopy (XPS) using a Kratos Axis Ultra DLD to examine the presence of iridium, oxygen, carbon and chlorine, and to look for any changes in film composition due to laser irradiation. Utah electrode impedances were measured by poking the electrodes into conductive agar using an impedance meter (Blackrock Microsystems). The agar was prepared from phosphate-buffered saline and agarose powder in a weight ratio of 42:1. A platinum counter electrode probe was inserted in the agar. Impedances of individual electrodes were measured sequentially using a probe signal of 100 nA (peak to peak) at a 1 kHz frequency.

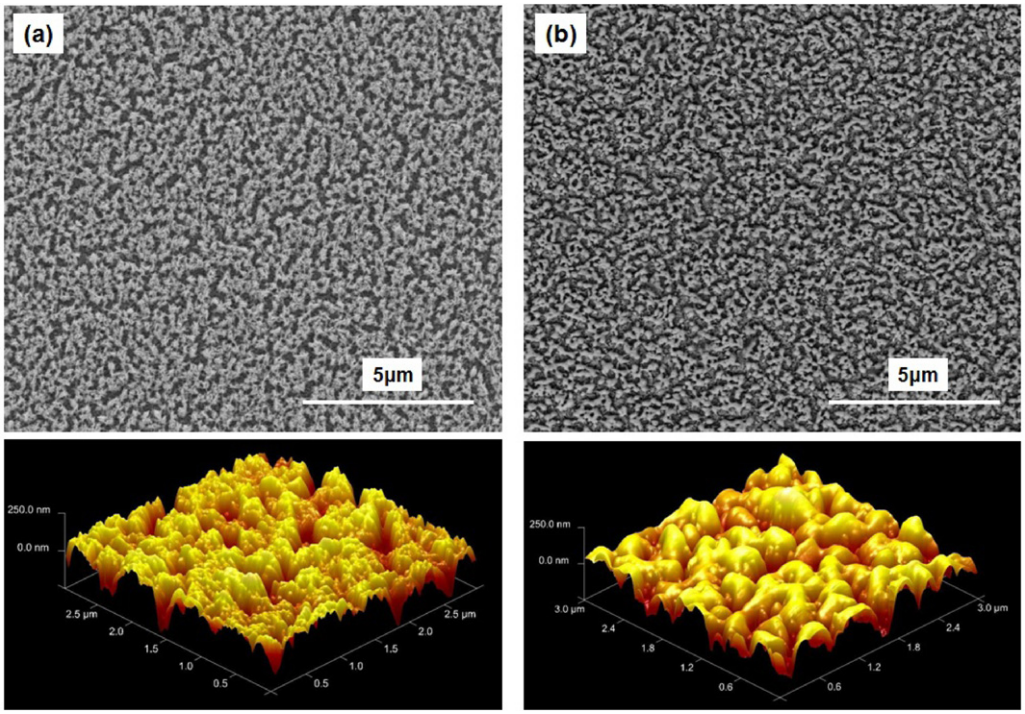

Fig. 7. SEM images (upper) and AFM images (bottom) of iridium oxide films before (left) and after (right) laser ablation.

3. Results and discussion

First, the effect of laser exposure after removal of the Parylene was investigated by changing the number of laser pulses. Fig. 4 shows a set of four SEM micrographs from a laser ablated hole in the Parylene film on the silicon substrate after laser ablation using a fluence of 1000 mJ/cm^2. When the number of pulses used for ablation was 10, the Parylene remained as a ripple-shaped circle as seen in Fig. 4(a). Figs. 4(b)–(d) have successively less Parylene remaining as the number of pulses was increased to 20, 30, and 100, respectively. Fig. 4(d) shows that a clean deinsulated surface without any Parylene residue was obtained when 100 pulses were used.

We then investigated the effect of beam fluence on the Parylene etch rate for the planar samples. Fig. 5(a) presents the etch depth of the Parylene film as a function of the number of pulses for 3.2 μm Parylene film. The last point of each curve indicates the number of pulses required to remove Parylene completely without any residue on the hole area. As expected, the number of pulses required for complete removal of Parylene decreased as a higher fluence was used. Fig. 5(b) shows the etch rate of Parylene as a function of the fluence, which indicates that at least approximately 250 mJ/cm^2 is required to etch Parylene.

The effect of SIROF thickness on the damage to the film from laser ablation was investigated. The incident laser energy absorbed in the surface material is converted into electronic or vibrational excitation energy, which causes laser desorption or ablation. The skin depth for excitation is typically on the order of tens of nanometers. Within a skin depth of about 50–100 nm of the surface, there is an extremely high density of excitation [14]. We compared several iridium oxide film samples with different thicknesses to investigate the film damage that is caused by laser energy. Fig. 6(a) shows the SEM images of iridium oxide films with three different thicknesses (0.4 μm, 0.8 μm, and 1.1 μm) after being exposed to a single laser pulse with 1680 mJ/cm^2 fluence. As can be seen in the figure, a thicker film had a higher resistance to damage. The threshold fluences for film damage were 1200, 1440, and 1920 mJ/cm^2 for the film thickness of 0.4 μm, 0.8 μm, and 1.1 μm, respectively. Additionally, the fluence and the number of pulses were also examined, and expected the iridium oxide film suffered from more fracture as higher laser fluence was used. However, the number of pulses did not show significant difference in film damage for up to 100 laser pulses as shown in Fig. 6(b). Based on these results, we chose the iridium oxide film thickness of 1.1 μm since it had a larger safety margin for clean removal of the Parylene without damaging the underlying iridium oxide film. Fig. 6(c) shows the SEM image of a laser deinsulated hole on a 1.1 μm thick iridium oxide film coated with 3 μm thickness of Parylene. The fluence and the number of pulses were 1000 mJ/cm^2 and 100, respectively. The image shows the deinsulated iridium oxide film without any damage.

The surface of an iridium oxide film was inspected using SEM and the data are presented in Fig. 7, with micrographs from (a) before and (b) after laser illumination. The surface became more granular after laser irradiation. Atomic force microscopy was also performed to examine the surface roughness of the iridium oxide film before and after the laser ablation. The left bottom image of Fig. 7 is the AFM image of an as-deposited iridium oxide film with the scan area of 3 μm × 3 μm and the R_{rms} of the film was 64 nm. The right bottom image of Fig. 7 shows the AFM images of an iridium oxide film with the same scan area after laser ablation and the R_{rms} of the film was 67 nm. However, when the scan area was reduced to 0.5 μm × 0.5 μm, the R_{rms} changed from 21.6 nm before laser ablation to 18 nm after laser ablation. This confirms that the surface of the iridium oxide film became smoother through heat treatment by laser energy.

To investigate change of the elemental/chemical composition of the iridium oxide surface during ablation, the XPS spectra using an Al Kα anode operated at 300 W and 15 kV were collected from the film from the 200 μm diameter ablated hole shown in Fig. 6. The XPS spectra from a bare Parylene film deposited on top of an iridium oxide film substrate show C1s and Cl 2p peaks as shown in the left of Fig. 8(a). The analysis area was approximately 700 μm × 300 μm. The XPS spectra from an ablated surface show Ir 4f and O 1s and C 1s peaks. The Ir 4d peak is very close to C 1s as can be observed in the right of Fig. 8(a). The XPS beam spot size was chosen as

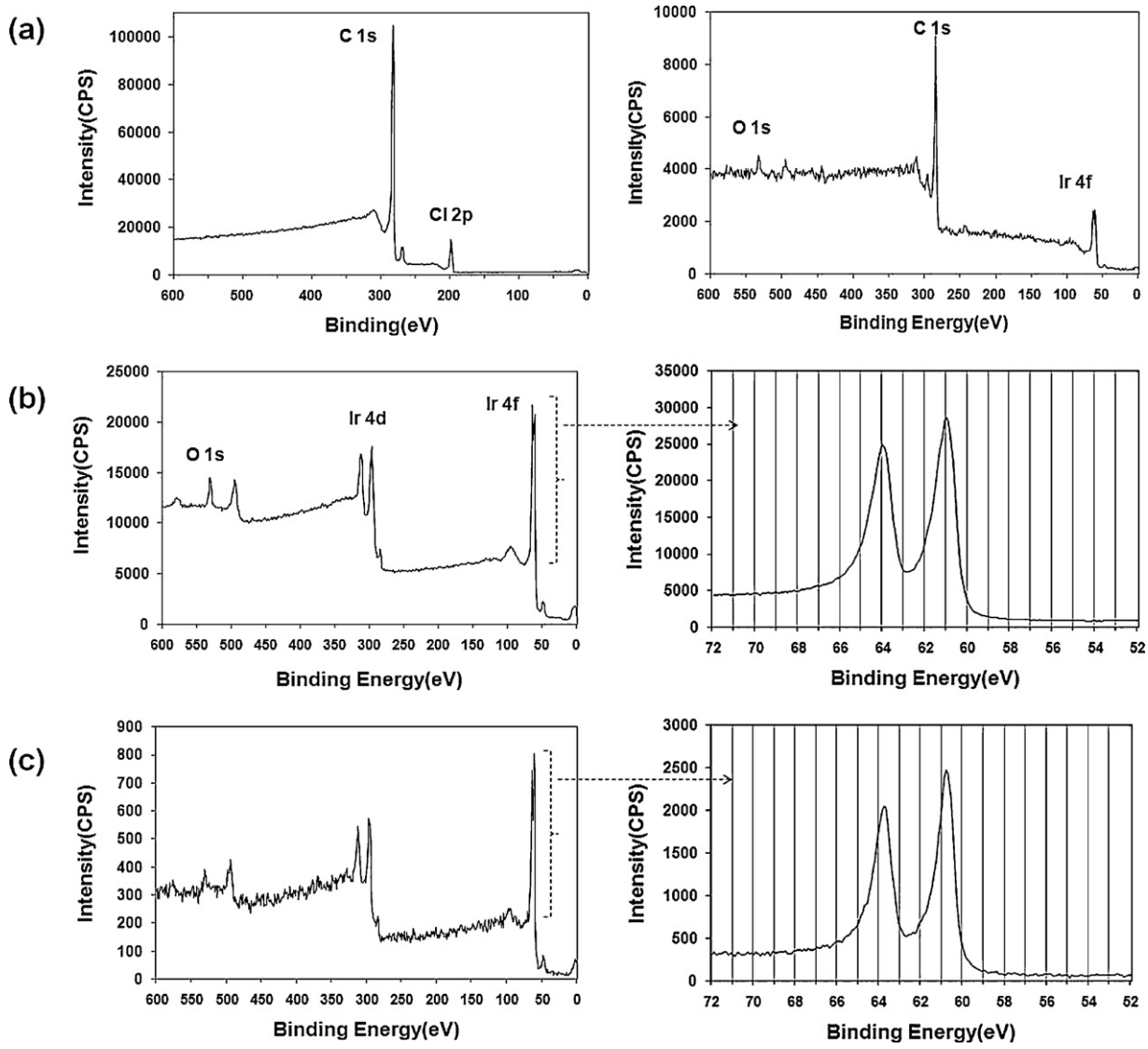

Fig. 8. X-ray photoemission spectra of (a) the Parylene film (left) and laser ablated spot on Parylene coated iridium oxide film (right), (b) as deposited iridium oxide film (left) and Ir 4f peaks in high resolution scan (right) and (c) laser ablated spot on as deposited iridium oxide film (left) and Ir 4f peaks in high resolution scan (right).

110 μm × 110 μm to analyze the ablated area of hole. The C 1s peak in the figure could be due to the debris of carbon coming onto the surface after the Parylene decomposition by the laser energy. During ablation, the molecular fragments ejected from the ablation zone could have the momentum exchange with the surrounding atmosphere and could have been redeposited on the ablated area. The redeposition occurs generally in vicinity of the ablation area. Although there are carbon deposits in the ablated area indicated by the C 1s peak, the absence of the chlorine peak indicates that the Parylene has been removed.

Fig. 8(b) and (c) presents XPS spectra of an as-deposited iridium oxide and a laser irradiated spot on the iridium oxide film. Both spectra show the Ir 4f and O 1s peaks. These peaks are similar to those observed in the right of Fig. 8(a) except for the carbon peak. The images on the right of Fig. 8(b) and (c) show the detailed Ir 4f peaks with high resolution which has very metallic characteristics. For the as-deposited iridium oxide shown in Fig. 8 (b) the peak position is 61 eV for Ir $4f_{7/2}$ and 64 eV for Ir $4f_{5/2}$. However, after laser ablation the position of the peaks shifted to the lower binding energy as shown in Fig. 8(c). This is attributed to the removal of the natural oxygen from the surface by laser energy. The XPS analysis shows that the laser ablation carried out in this experiment did not change elemental/chemical composition of the iridium oxide.

Finally, the laser tip deinsulation was performed on the 3-D Utah electrode array. The thickness of the iridium oxide film was 1.1 μm, which was determined from prior experimental data on the planar structure as described previously. The electrode tip exposure should be targeted at more than 20 μm from the tip of the electrode to the encapsulation edge in the Utah electrode to acquire good neuron sensitivity and impedance value enough for neural recording applications in cortical tissue [6]. Fig. 9 shows 30° tilted scanning electron micrograph images of a Utah electrode tip with 1.1 μm thick iridium oxide film after laser illumination. Fig. 9(a) shows the images of laser deinsulated tips after they were exposed to 35, 100, and 200 laser pulses with a fluence of 1440 mJ/cm^2. The exposures of the electrode tip to the encapsulation edge are ~5, 30, and 90 μm for 35, 100, and 200 laser pulses, respectively. Fig. 9(b) shows the images of laser deinsulated tips after they were exposed to the fluence of 1200, 1440, and 1680 mJ/cm^2 with 150 laser pulses. The exposures of the electrode tip to the encapsulation edge are ~45, 60 and 80 μm for the fluence of 1200, 1440, and 1680 mJ/cm^2, respectively. These results indicate that the exposure of the electrode tip can be controlled by fluence and number of

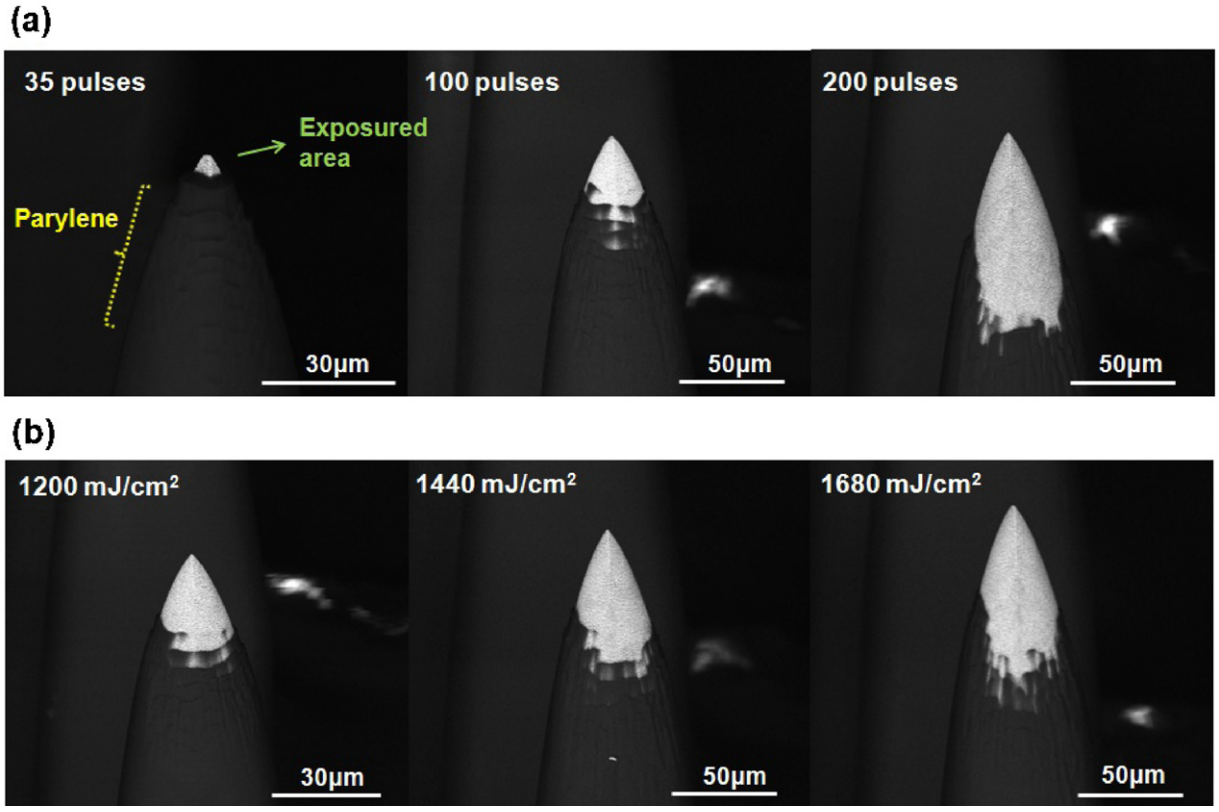

Fig. 9. 30° tilted scanning electron micrograph using backscattered electron images of a Utah electrode tip having 1.1 μm thickness iridium oxide film after laser deinsulation by (a) 35, 100, and 200 pulses with the fluence of 1440 mJ/cm^2 and (b) fluence of 1200, 1440, and 1680 mJ/cm^2 with 150 laser pulses.

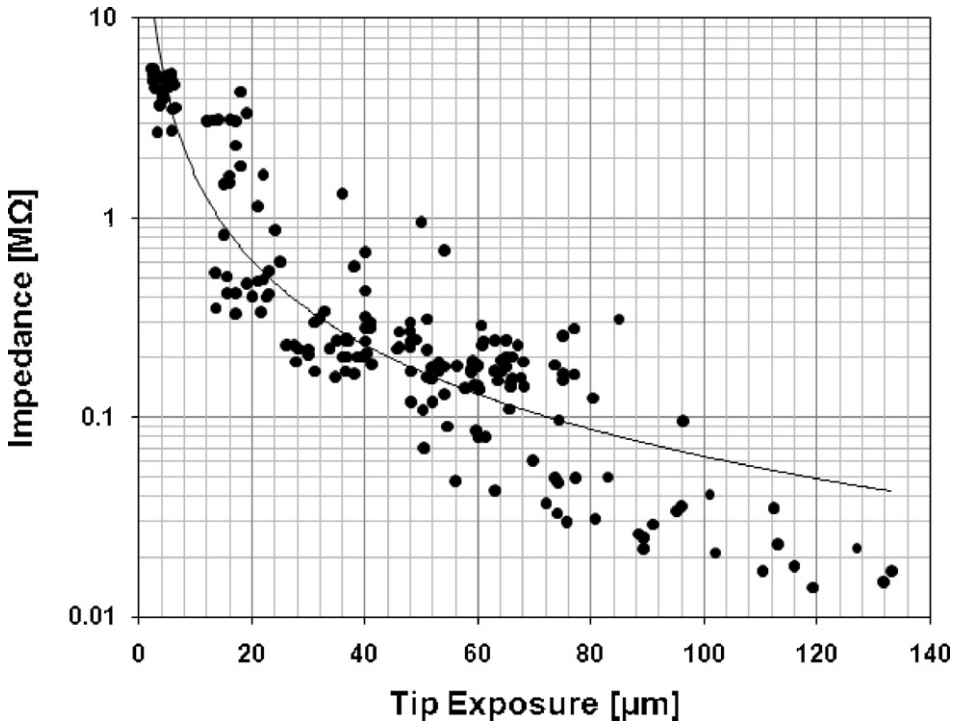

Fig. 10. Impedance values as a function of the tip exposure of laser deinsulated Utah electrode. The tip exposure lengths were measured by SEM at a 30° sample tilt angle. The solid line is the trend line with the equation $y = 41.309x^{-1.406}$.

laser pulses. The uneven removal of Parylene from the electrode tips is attributed to the nonuniformity of laser power and the varying oblique angles between the laser beam and the electrode tip surface. However, the tip exposure was highly reproducible, leading to the same area of exposure under the same deinsulation conditions.

Fig. 10 shows the impedance values as a function of the tip exposure of laser deinsulated Utah electrode arrays. The *y*-axis is a log scale to express the impedance value in the entire tip exposure range from ~2 μm to ~130 μm. The tip exposure lengths were measured by SEM at a 30° sample tilt angle. The solid line is the trend line with the equation $y = 41.309x^{-1.406}$. The impedance value became around 0.02 MΩ as the tip exposure is increased beyond 140 μm and become larger than 1 MΩ for tip exposures of less than 20 μm. The rather high deviation of impedance values from the trend line is attributed to the variation of the contact force of the working probe during impedance measurement and the variation of the amount of carbon redeposition on the active tip surface during the laser ablation process. The electrode tip exposure larger than 100 μm provides the impedance value of a few tens of kilo-ohm, which is the normal target impedance value for neural interface applications [6].

4. Conclusions

This study demonstrated that the laser ablation using a KrF excimer laser is an effective deinsulation method for Parylene-coated Utah electrode array. Optimum conditions for deinsulating the electrode tips in the UEA using the laser ablation were investigated through XPS, SEM, and AFM analyses and impedance measurement. The thickness of the iridium oxide film that is resistant to the film fracture induced by laser energy was derived and the parameters of laser ablation in terms of the fluence and the number of laser pulses for complete removal of Parylene film from the electrode tip were also derived. The laser ablation process was used for deinsulation of Parylene-coated Utah electrode array, producing the electrode impedance in the range of tens of kΩ that is suitable for implantable neural interface device applications. A more sophisticated method to remove the residual carbon redeposited on the deinsulated electrode surface will be explored to reduce the rather large variation of the electrode impedance value. The results suggest that the laser ablation using a KrF excimer laser is acceptable for deinsulation of the Utah electrode tips and more complicated electrode structures for implantable device applications.

Acknowledgments

This work was supported by WCU (R31-2008-000-10026-0) and Bio-imaging Research Center programs at GIST, and DARPA award N66001-06-C-4056. Sample fabrication, laser deinsulation, and film characterization were performed in the Utah Nanofabrication Lab and the Surface and NanoImaging Lab at University of Utah. I would like to thank Brian van Devener, Kathryn Ecsedy, and others for assistance in collecting XPS and SEM data and the UEA production team for providing the electrode arrays. Florian Solzbacher has commercial and financial interest in Blackrock Microsystems.

References

[1] C. Hassler, R.P. von Metzen, P. Ruther, T. Stieglitz, Characterization of parylene C as an encapsulation material for implanted neural prostheses, Journal of Biomedical Materials Research Part B: Applied Biomaterials 93B (2010) 266–274.
[2] G.E. Loeb, M.J. Bak, M. Salcman, E.M. Schmidt, Parylene as a chronically stable, reproducible microelectrode insulator, biomedical engineering, IEEE Transactions on BME 24 (1977) 121–128.
[3] D.C. Rodger, A.J. Fong, W. Li, H. Ameri, A.K. Ahuja, C. Gutierrez, I. Lavrov, H. Zhong, P.R. Menon, E. Meng, J.W. Burdick, R.R. Roy, V.R. Edgerton, J.D. Weiland, M.S. Humayun, Y.-C. Tai, Flexible parylene-based multielectrode array technology for high-density neural stimulation and recording, Sensors and Actuators B: Chemical 132 (2008) 449–460.
[4] R.A. Normann, Technology insight: future neuroprosthetic therapies for disorders of the nervous system, Nature Clinical Practice. Neurology 3 (2007) 444–452.
[5] E. Meng, et al., Plasma removal of Parylene C, Journal of Micromechanics and Microengineering 18 (2008) 045004.
[6] H. Jui-Mei, L. Rieth, R.A. Normann, P. Tathireddy, F. Solzbacher, Encapsulation of an integrated neural interface device with parylene C, IEEE Transactions on Biomedical Engineering 56 (2009) 23–29.
[7] P.K. Campbell, K.E. Jones, R.J. Huber, K.W. Horch, R.A. Normann, A silicon-based, three-dimensional neural interface: manufacturing processes for an intracortical electrode array, IEEE Transactions on Biomedical Engineering 38 (1991) 758–768.
[8] J. Ji, et al., Microfabricated microneedle with porous tip for drug delivery, Journal of Micromechanics and Microengineering 16 (2006) 958.
[9] R. Bhandari, S. Negi, L. Rieth, R.A. Normann, F. Solzbacher, A novel masking method for high aspect ratio penetrating microelectrode arrays, Journal of Micromechanics and Microengineering 19 (2009) 035004.
[10] M. Esashi, M. Minami, S. Shoji, Optical exposure systems for three-dimensional fabrication of microprobe, in: Micro Electro Mechanical Systems MEMS '91, Proceedings. An Investigation of Micro Structures, Sensors, Actuators, Machines and Robots. IEEE, 1991, pp. 39–44.
[11] G.E. Loeb, R.A. Peck, J. Martyniuk, Toward the ultimate metal microelectrode, Journal of Neuroscience Methods 63 (1995) 175–183.
[12] E.M. Schmidt, M.J. Bak, P. Christensen, Laser exposure of Parylene-C insulated microelectrodes, Journal of Neuroscience Methods 62 (1995) 89–92.
[13] C. Yoonsu, O.C. Seong, R.H. Shafer, M.G. Allen, Highly inclined electrodeposited metal lines using an excimer laser patterning technique, in: Digest of Technical Papers. TRANSDUCERS '05. The 13th International Conference on Solid-State Sensors, Actuators and Microsystems, vol. 1462, 2005, pp. 1469–1472.
[14] J.C. Miller, R.F. Hagulnd, Laser Ablation and Desorption, Academic Press, 2009.
[15] R. Bhandari, S. Negi, L. Rieth, F. Solzbacher, A wafer-scale etching technique for high aspect ratio implantable MEMS structures, Sensors and Actuators A: Physical 162 (2010) 130–136.

Biographies

Je-Min Yoo received his Master's degree in Physics in 2006 at Korea University. In 2007, he started his Ph.D. degree in the Department of Nanobio Materials and Electronics in Gwangju Institute Science and Technology. He has worked in the Integrated Neural Interface Program (INIP) at the University of Utah as a visiting researcher since 2009. His current research interests include the design, fabrication, testing of MEMs and wireless Brain Machine Interface (BMI) devices, power/data transfer system, and CMOS analog circuit design.

Asha Sharma received her Ph.D. from the Indian Institute of Technology Kanpur, India, in 2006. She was a Postdoctoral Fellow at the Georgia Institute of Technology in Atlanta in the School of ECE until 2008. Following that, she worked at the University of Utah in Salt Lake City from 2009 to 2011 as a Postdoctoral Researcher in the Microsystems Laboratory, focusing her research on fully integrated wireless neural interfaces. She is currently a Research Scientist-II at the Georgia Institute of Technology in Atlanta in the School of ECE. Her primary research interests are organic electronic devices, such as OPV, OLED, and OFET. In addition, she is also interested in the application of organic electronics and photonics to the biology and medicine for the next generation of biocompatible, low cost, and clean-environment healthcare technologies. She has co-authored 23 publications in peer-reviewed journals and 24 contributed conference presentations and proceedings.

Prashant Tathireddy received a Bachelor's degree in chemical technology from Osmania University, Hyderabad, India, in 1997, and the Ph.D. degree from the Department of Chemical Engineering, University of Utah, Salt Lake City, in 2004. Until 1999, he was a Project Leader at Computer Maintenance Corporation (CMC) Limited, Hyderabad. Until 2007, he was a Postdoctoral Fellow in the Microsystems Laboratory, Department of Electrical and Computer Engineering, University of Utah, where he is currently a Research Assistant Professor in the Department of Electrical and Computer Engineering. He is also a Guest Scientist at Fraunhofer Institute for Biomedical Engineering (IBMT) in St. Ingbert, Germany. His current research interests include development and fabrication of implantable microdevices (BioMEMS), microfluidics, and microsensors.

Loren Rieth received his BS degree in materials science from The Johns-Hopkins University, Baltimore, MD, in 1994. He received his PhD in materials science and engineering from the University of Florida, Gainesville, FL, in 2001. From 2001 to 2003, he was a postdoctoral research associate at the University of Utah, Salt Lake City, UT, and continued at the University of Utah as a research assistant professor in materials science (2003–2005), and electrical and computer engineering (2004–present). His research is focused on deposition and characterization of thin film materials for sensors (chemical, physical, and biological), MEMS, BioMEMS, and energy production.

Florian Solzbacher received his MSc. in electrical engineering from the Technical University Berlin in 1997 and his Ph.D. from the Technical University Ilmenau in 2003. He is director of the Microsystems Laboratory at the University of Utah and a faculty member in the departments of Electrical and Computer Engineering,

Materials Science and Bioengineering, and he is responsible for the Utah branch office of the Fraunhofer IZM, Germany. Dr. Solzbacher is co-founder of First Sensor Technology GmbH, an established supplier to the automotive and process control industry in the USA, Europe and Asia. He is Chairman of the German Association for Sensor Technology AMA. His work focuses on harsh environment microsystems, sensors and materials. He is author of over 60 scientific and engineering publications and book chapters on MEMS devices, technologies and markets for harsh environments. Since 2004, he has been Chairman of Sensor + Test, the world's largest international trade fair and ensemble of conferences for sensors, metrology and testing.

Jong-In Song received the BS degree in electronics engineering from Seoul National University, Seoul, Korea, in 1980, the MS degree in electronics engineering from the Korea Advanced Institute of Science and Technology (KAIST), Daejon, Korea, in 1982, and the Ph.D. degree in electrical and electronics engineering from Columbia University, New York, NY, in 1990. From 1986 to 1990, he was a Graduate Research Assistant with the Center for Telecommunications Research, where he pioneered high-performance GaAs/AlGaAs 2-D electron gas (2DEG) charge coupled device research for microwave and infrared-imaging applications. From 1990 to 1994, he joined the Electronics Science and Technology Division, Bellcore, where he was primarily involved in the development of microwave transistors including GaInP/GaAs, InAlAs/InGaAs, InP/InGaAs HBTs, and their application to monolithic microwave integrated circuits (MMICs). In 1994, he joined the Gwangju Institute of Science and Technology (GIST), Gwangju, Korea, where he is currently a Professor with the Department of Nanobio Materials and Electronics. His current research interests include low-power and high-speed devices and circuits, millimeter-wave over fiber (MMoF) communication systems, and distributed sensor networks.

UU IR Author Manuscript